Journal of
Developmental Biology

MDPI

Article

Discovery of New Markers for Haemogenic Endothelium and Haematopoietic Progenitors in the Mouse Yolk Sac

Guillermo Diez-Pinel [1], Alessandro Muratore [1,2], Christiana Ruhrberg [1,*] and Giovanni Canu [1,*]

[1] UCL Institute of Ophthalmology, University College London, London EC1V 9EL, UK; guillermo.pinel.21@ucl.ac.uk (G.D.-P.); a.muratore@campus.unimib.it (A.M.)
[2] School of Medicine and Surgery, University of Milano-Bicocca, 20900 Monza, Italy
* Correspondence: c.ruhrberg@ucl.ac.uk (C.R.); g.canu@ucl.ac.uk (G.C.)

Abstract

Erythro-myeloid progenitors (EMPs) originate from the haemogenic endothelium in the yolk sac via an endothelial-to-haematopoietic transition (EHT) to generate blood and immune cells that support embryo development. Yet, the transitory nature of EHT and the limited availability of molecular markers have constrained our understanding of the origin, identity, and differentiation dynamics of EMPs. Here, we have refined the annotation of yolk sac haemato-vascular populations in publicly available single-cell RNA sequencing (scRNAseq) datasets from mouse embryos to identify novel molecular markers of haemogenic endothelium and EMPs. By sub-clustering key cell populations followed by pseudotime analysis, we refined cluster annotations and then reconstructed differentiation trajectories. Subsequent differential gene expression analysis between clusters identified novel cell surface markers for haemogenic endothelial cells (*Fxyd5* and *Scarf1*) and EMPs (*Fcer1g*, *Tyrobp*, and *Mctp1*). Further, we have identified candidate signalling and metabolic pathways that may regulate yolk sac haematopoietic emergence and differentiation. The specificity of FXYD5, SCARF1, and FCER1G for haemogenic endothelium and EMPs was validated by immunostaining of the mouse yolk sac. These insights into the transcriptional dynamics in the yolk sac should support future investigation of EHT and haematopoietic differentiation during early mammalian development.

Keywords: haemogenic endothelium; erythro-myeloid progenitors; EMPs; haematopoietic development; haematopoietic differentiation; yolk sac; mouse embryo; single-cell transcriptomic; Fxyd5/Dysadherin; Scarf1; Fcer1g

Academic Editors: Jianhang Jia, Junichi Iwata and Simon J. Conway

Received: 7 November 2025
Revised: 26 December 2025
Accepted: 30 December 2025
Published: 6 January 2026

1. Introduction

Haematopoiesis in the developing embryo proceeds in three temporally and spatially overlapping waves in proximity to vascular endothelial cells [1,2]. The first wave, known as primitive haematopoiesis, arises in the yolk sac when extra-embryonic mesoderm differentiates into vascular and haematopoietic progenitors that progressively organise into blood islands and produce nucleated erythrocytes, megakaryocytes, and macrophages [3]. This process occurs in the mouse from embryonic day (E) 7.0 onwards, equivalent to 2–3 post-conception weeks in humans.

The second haematopoietic wave, known as pro-definitive or transient definitive haematopoiesis, also emerges in the yolk sac, when a change in cellular identity causes haematopoietic progenitors to bud off the endothelium as clusters of round cells, a process

called endothelial-to-haematopoietic transition (EHT) [4]. In the mouse yolk sac, EHT generates mainly erythro-myeloid progenitors (EMPs) from E8.5, alongside lympho-myeloid progenitors (LMPs) from E9.5 [5,6]. Once the blood circulation is established by E9.5, these progenitors are transported out of the yolk sac and seed the foetal liver, from where they contribute blood and immune cells from mid-gestation until birth [7]. Additionally, we recently showed that haematopoietic progenitors akin to EMPs can also arise from a *Pax3*-expressing lineage in the mouse and transiently seed the foetal liver by E12.5 to contribute erythroid and myeloid cells to foetal haematopoiesis [8]. Based on their origin from a *Pax3*-expressing progenitor, these haematopoietic cells may arise via EHT from a paraxial mesoderm-derived haemogenic endothelium, although further work is needed to address this possibility. Among the early haematopoietic populations, yolk sac-derived EMPs generate blood and immune cells important for embryogenesis [5,7] and self-renewing tissue-resident macrophages that persist into adulthood [9–11].

The third haematopoietic wave, known as definitive haematopoiesis, originates intra-embryonically in the dorsal aorta, where EHT produces haematopoietic stem cells (HSCs) that enter the circulation to first colonise the foetal liver by mid-gestation and later seed the bone marrow to establish long-term, self-renewing adult haematopoiesis [1,12–16]. HSCs are first produced at E10.5 in the mouse and 4–5 post-conception weeks in humans.

Despite their key roles in embryonic haematopoiesis and the generation of tissue macrophages with a role in adult homeostasis, the transitory nature of EMPs and their overlapping markers with HSC lineages have made the study of EMP-derived cell lineages challenging. For example, the Lin^- KIT^+ $CD41^{low}$ $CD16/32^+$ cell surface profile allows EMP isolation by flow cytometry from the early embryo but is insufficient to unambiguously distinguish EMPs from HSC-derived myeloid progenitors at mid-gestation [17,18]. Temporally controlled lineage tracing via Cre-mediated reporter gene activation has therefore been used as a complementary approach to distinguish EMPs from HSC-derived progenitors based on the earlier production of EMPs [7,19,20]. However, this approach relies on transgenic mice expressing suitable Cre drivers and expression reporters. Therefore, specific molecular markers are needed to allow accurate EMP isolation and to study their formation and behaviour in the mouse embryo. Moreover, such markers might facilitate the identification of analogous markers suitable to study foetal haematopoiesis in human embryos, in which genetic lineage tracing is not an option.

Here, we have leveraged publicly available mouse embryonic single-cell RNA sequencing (scRNAseq) data to investigate cell populations in the developing mouse yolk sac to identify novel candidate markers for haemogenic endothelium and EMPs.

2. Methods

2.1. Integration of Publicly Available E8.5 scRNAseq Mouse Embryo Data

The file 'embryo_sce.rds' containing a processed SingleCellExperiment object including scRNAseq data from the ArrayExpress dataset E-MTAB-6967 [21] and ArrayExpress dataset E-MTAB-11763 [22] was downloaded from https://marionilab.github.io/ExtendedMouseAtlas/ (last accessed on 25 August 2025). The cells annotated as embryonic day E8.5 were subset for analysis in R v4.5.1, with Rstudio v2025.05.1 using the Seurat v4.5.1 R package [23]. The function 'as.Seurat' was used to generate a Seurat object from the SingleCellExperiment object. For sample integration, the E-MTAB-11763 cells were subset and split into layers containing individual samples. Counts were log-normalised with the 'NormalizeData' function, the top 2000 variable features were identified with 'FindVariableFeatures', and were scaled and centred with the 'ScaleData' function. Then, PCA dimensionality reduction was performed with the 'RunPCA' function, and Harmony Integration [24] was performed using the 'IntegrateLayers' function. A Uniform Mani-

fold Approximation and Projection (UMAP) reduction was obtained with the 'RunUMAP' function, for which the number of principal components was selected by examination of an elbow plot. Lastly, the layers were joined with the 'JoinLayers' function. This same integration pipeline was used for all other data integration in the study.

2.2. Re-Annotation of Yolk Sac Cell Types in E8.5 scRNAseq Data

Cells with anatomy 'Yolk sac' (YS) from haemato-vascular cell types were subset and integrated by sample. For clustering, a k-nearest neighbour (KNN) graph was calculated (k = 20), and the Louvain algorithm was used for graph clustering. Then, the expression of known cell type markers in the yolk sac clusters was used alongside the anatomical origin (yolk sac or embryo) to annotate these haemato-vascular yolk sac cells, as well as the embryo haemato-vascular cells, more accurately. Afterward, both yolk sac and embryo cells were merged and integrated by sample. These data were then used as the reference dataset for reference-based annotation of the E-MTAB-6967 haemato-vascular cells using the SingleR v2.10.0 R package [25], and then merged and integrated by sample with the E-MTAB-11763 data.

2.3. Analysis of Gene Expression Along the EHT Differentiation Trajectory

To identify haemogenic endothelium cells, we sub-clustered all cells annotated as endothelial cells and EMPs in the combined dataset, including allantois endothelium, venous endothelium, embryo proper endothelium, endocardium, YS endothelium, vitellin vein endothelium, EMPs, and EMP-like embryo, and then examined the expression of haemato-vascular markers. To analyse the EHT differentiation trajectory, we sub-clustered yolk sac haemato-vascular cells, including YS endothelium, haemogenic endothelium, EMPs, BP1, BP2, and erythroid, and the resulting UMAP reduction was used to carry out a pseudotime analysis to predict differentiation trajectories with the Monocle3 v1.4.26 R package [26]. Genes that changed as a function of pseudotime were identified with the 'graph_test' function, and were grouped with the 'find_gene_modules' function according to their expression patterns into modules, which were then grouped manually into four supermodules (downwards trend, upwards trend, peaking at EMPs, and peaking at BP1).

2.4. Gene Ontology and Differential Gene Expression of Haemato-Vascular Clusters

Enrichment analyses against the GeneOntology: Biological Pathway and WikiPathways databases were carried out using the 'enrichGO' and 'enrichWP' functions from the clusterProfiler v4.16.0 R package [27], respectively. All genes with at least 1 count were used as the background universe. Cytoscape 3.10.3 [28] and the RCy3 v2.28.1 R package [29] were used to plot the TYROBP WikiPathway pathway. For surface marker identification, differential expression analyses were carried out with the 'FindMarkers' function, with an adjusted P-value threshold of 0.05. Then, Uniprot accession IDs were retrieved from the org.Mm.eg.db v3.21.0 R package [30] using the 'select' function from the AnnotationDbi v1.70.0 R package [31]. A list of curated transmembrane proteins was obtained from Uniprot (https://www.uniprot.org/) on 30 July 2025 using the query '(keyword:KW-0812) AND (reviewed:true)' and filtering for 'Mouse' as the relevant organism. This list was then used to filter the differential expression results for transmembrane proteins. Plotting of UMAP reductions was carried out with Seurat's 'DimPlot' and the function 'DimPlot_scCustom' from the scCustomize v3.2.0 package [32]. Plotting of normalised gene expression onto UMAP reductions was carried out with Seurat's 'FeaturePlot' and scCustomize's 'FeaturePlot_scCustom' functions. Other plots were generated using the ggplot2 v4.0.0 R package [33].

2.5. Animal Procedures and Tissue Staining

Animal procedures were performed with Animal Welfare Ethical Review Body (AWERB) and UK Home Office approval. C57BL/6J mice were timed-mated for embryo collection at E8.5 after cervical dislocation and culling of the pregnant dam. Yolk sacs were fixed in 4% formaldehyde, washed in phosphate-buffered saline (PBS) and then blocked in PBS containing 2% serum-free protein block (DAKO), 2% bovine serum albumin and 0.4% Triton X-100 before staining with the following antibodies: goat anti-mouse KIT (R&D Systems, Abingdon, UK #AF1356-SP, 1:50), rat anti-mouse PECAM1 (BD Pharmingen, Wokingham, UK #553370, 1:50), rabbit anti-mouse FXYD5/Dysadherin (Proteintech, Manchester, UK #12166-1-AP, 1:50), rabbit anti-mouse SCARF1 (Proteintech, Manchester, UK #13702-1-AP, 1:100) or rabbit anti-mouse FCER1G (GeneTex, Wembley, UK #GTX108487s, 1:50), followed by the appropriate secondary antibodies, which were Alexa Fluor 488-conjugated donkey anti-goat Fab fragments (Stratech, Cambridge, UK #705-547-003, 1:200), Cy3-conjugated donkey anti-rat Fab fragments (Stratech, Cambridge, UK #712-166-150, 1:200), and Alexa Fluor 647-conjugated donkey anti-rabbit Fab fragments (Stratech, Cambridge, UK #711-607-003, 1:200). Secondary-only controls were included. DAPI-counterstained sections were imaged on a LSM710 confocal microscope (Zeiss, Cambridge, UK).

3. Results

3.1. Refined Annotation of E8.5 Yolk Sac and Embryo Cell Clusters

To identify the transcriptomic signature of yolk sac haemogenic endothelium and that of its haemopoietic progeny, we re-analysed published scRNAseq data from E8.5 mouse embryos (Figure 1A), which were extracted from the ArrayExpress datasets E-MTAB-6967 [21] and E-MTAB-11763 [22]. E-MTAB-6967 contains data from E6.5 to E8.5 mouse embryos, including yolk sac and embryo proper, which were sequenced and analysed together to construct a molecular atlas describing early mouse gastrulation [21]. E-MTAB-11763 instead contains data that were generated by collecting yolk sac and embryo proper from E8.5 to E9.5 mouse embryos and sequencing them separately. These two published datasets overall comprise 400,000 cells from E6.5 to E9.5. A subsequent in silico merge of E-MTAB-11763 data and E-MTAB-6967 embryo and yolk sac data was previously analysed to compare the mouse versus human yolk sac contribution to metabolic and nutritional support, as well as to early erythroid and myeloid lineages [22]. As the goal of our analysis was to define the transcriptome of yolk sac endothelium and its haematopoietic progeny at the time when EMPs emerge from yolk sac haemogenic endothelium, we subset only the E8.5 data from E-MTAB-6967 and E-MTAB-11763 (Figure 1A).

First, we analysed E8.5 data from E-MTAB-11763, which contained yolk sac and embryo proper data annotated separately, and generated a UMAP including 75 clusters, using the cluster annotations provided by the authors of the original publication (Figure S1). Next, we selectively sub-clustered the 8453 haemato-vascular cells that had been sequenced from the yolk sac (Figure 1B,C). To confirm the identity of the resulting clusters, we analysed the expression of known markers of endothelial and haematopoietic progenitor populations (Figure 2A–D). The yolk sac endothelial cell (EC) cluster was identified via expression of the pan-EC markers *Kdr* and *Cdh5* together with *Lyve1* and *Stab2* (Figure 2A) as two markers typical for yolk sac ECs [34,35]. The EMP cluster was identified via detection of *Csf1r* and *Ptprc* as well as the myeloid markers *Spi1* and *Mpo* (Figure 2B). Notably, *Kdr*, *Cdh5*, and *Lyve1* were also detected in the EMP cluster (Figure 2A), agreeing with their known endothelial origin [20]. Clusters expressing haematopoietic progenitor markers (*Vav1*, *Myb*, and *Gata2*) (Figure 2C) together with erythroid (*Gata1* and *Klf1*) or myeloid (*Spi1* and *Mpo)* differentiation markers (Figure 2D) represented intermediate progenitors at different

states of commitment and were annotated as blood progenitors (BP) 1 and BP2 (Figure 1C). Finally, high expression levels of differentiation markers (*Alas2* and *Gypa*) (Figure 2D), in the absence of endothelial (*Cdh5* and *Lyve1*), EMP (*Csf1r* and *Ptprc*), or progenitor markers (*Spi1* and *Gata2*), identified a cluster of differentiated erythroid cells.

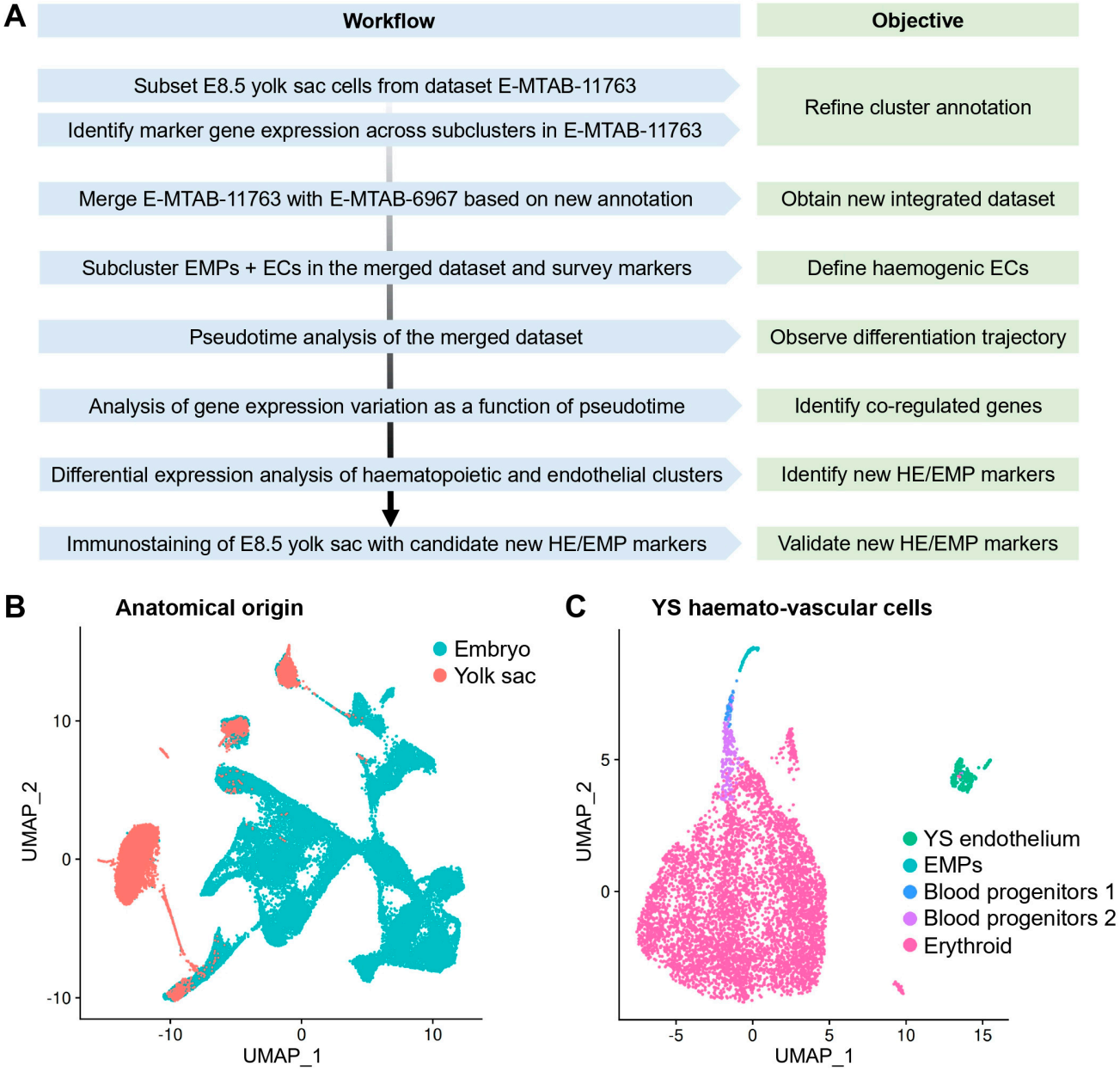

Figure 1. Re-analysis of E8.5 mouse embryonic scRNAseq data to study yolk sac EHT. (**A**) Workflow for the integrated re-analysis of mouse embryonic scRNAseq datasets E-MTAB-11763 and E-MTAB-6967. (**B**) UMAP of dataset E-MTAB-11763 showing cells sequenced from the E8.5 mouse embryo and labelled according to their anatomical origin as embryo and yolk sac. (**C**) UMAP obtained by subsetting haemato-vascular cells from the E8.5 yolk sac from E-MTAB-11763 and labelled based on our refined cluster annotation. EMP: erythro-myeloid progenitor; EC: endothelial cell; HE: haemogenic endothelium; YS: yolk sac.

As expected, the detection levels of endothelial and haematopoietic genes displayed opposite trends between the endothelial and haematopoietic clusters. Thus, *Kdr* and *Cdh5* appeared highly expressed in ECs and EMPs, but their detection declined in BP1, whilst they were barely detectable in BP2 and absent from erythroid cells (Figure 2A). Conversely,

erythroid genes such as *Klf1* and *Gypa* were not detected in ECs and EMPs but were detected at low levels in BP1, at higher levels in BP2, and at very high levels in erythroid cells (Figure 2D). Known haematopoietic progenitor markers (e.g., *Myb*, *Gata2*, and *Runx1*) displayed a gradual decrease from EMPs to BP1 and BP2, supporting the notion that the three clusters represented successive maturation stages (Figure 2C). Myeloid markers (e.g., *Csf1r*, *Spi1*, and *Mpo*) did not identify a separate cluster but were present in the EMP cluster and, at lower levels, also in BP1 (Figure 2B), agreeing with prior studies suggesting that macrophages are only present in the yolk sac from E9.0 onwards [36].

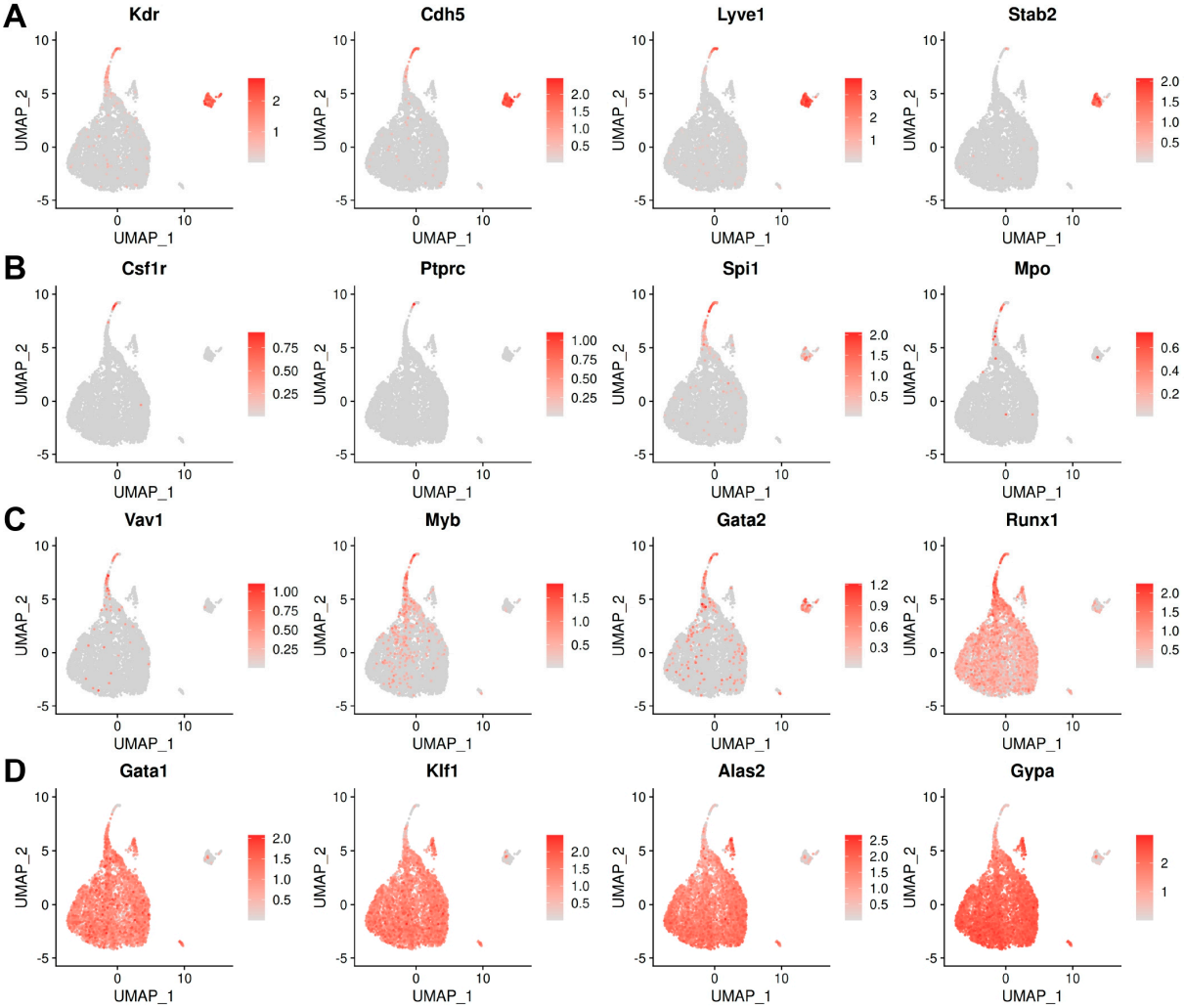

Figure 2. Marker analysis identifies haemato-vascular cell populations in E8.5 yolk sac data in E-MTAB-11763. UMAP representation of transcript levels for the indicated marker genes for (**A**) endothelial cells, (**B**) EMPs, (**C**) haematopoietic progenitors, and (**D**) erythroid cells. The scale bar represents log-normalised transcript levels.

Unexpectedly, we observed that E-MTAB-11763 contained cells that had been isolated and sequenced from the embryo proper but nevertheless clustered with yolk sac EMPs and BPs; accordingly, we annotated these cells as EMP-like embryo and blood progenitors embryo, respectively (Figure 3A,B). Also unexpectedly, some cells sequenced from the embryo proper had been annotated in the original publication describing E-MTAB-11763 as representing yolk sac-derived ECs. As the endothelium in the yolk sac vasculature forms a continuum with the endothelium of the vitelline vein, cells within the embryo proper that resemble yolk sac ECs likely represent vitelline vein ECs, and we re-annotated them accordingly (Figure 3A,B).

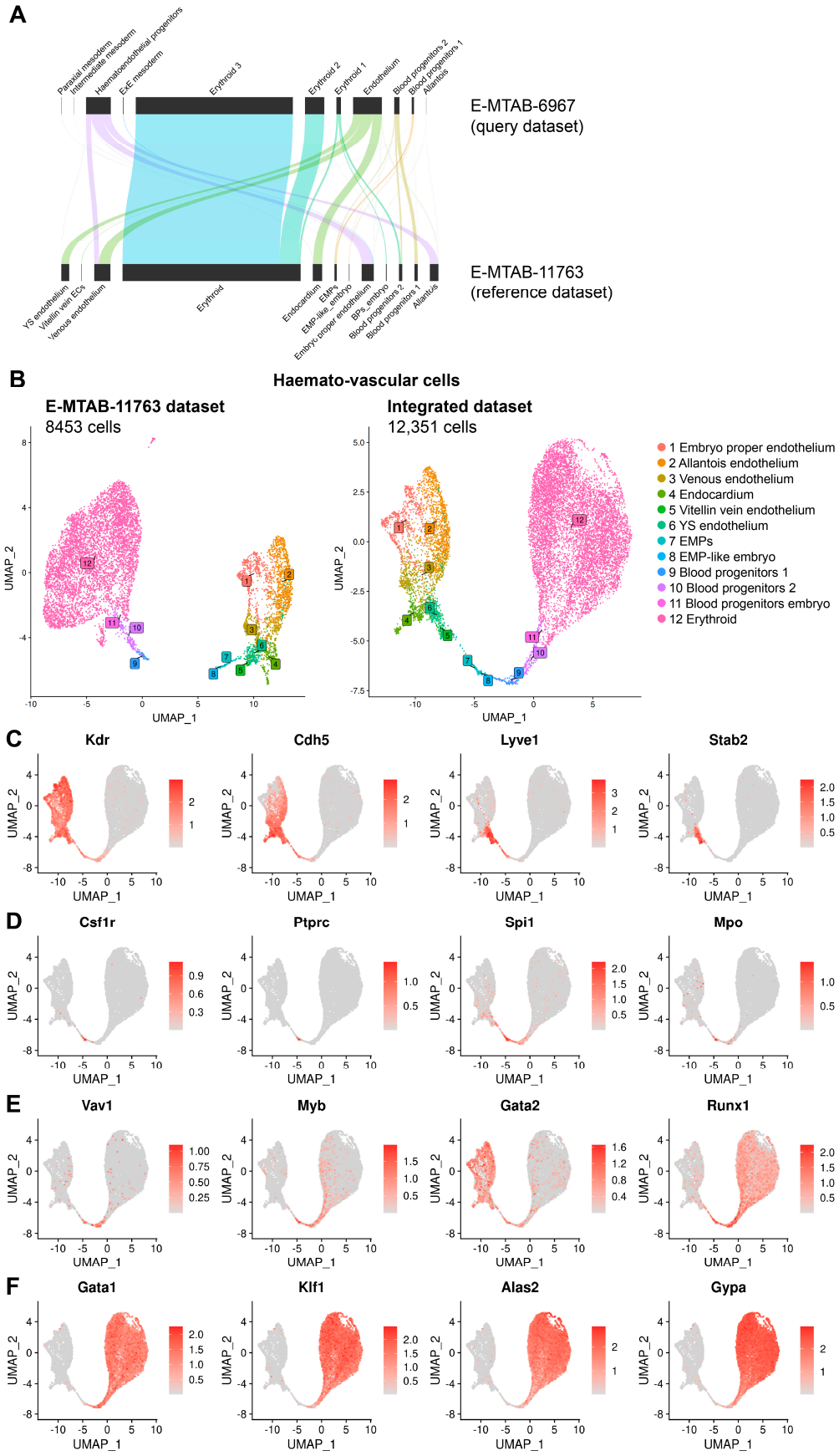

Figure 3. Refined cluster annotation of E8.5 embryo and yolk sac haemato-vascular cell clusters after integration of E-MTAB-11763 and E-MTAB-6967. (**A**) Reference-based annotation based on gene expression was used to apply our revised annotation for E8.5 data in E-MTAB-11763 to the E8.5 data

in E-MTAB-6967 before integrating the two datasets. (**B**) UMAPs showing the E8.5 haemato-vascular clusters from both embryo and yolk sac for dataset E-MTAB-11763 before integration to dataset E-MTAB-6967 and after reference-mapping and integration of the two datasets. (**C**–**F**) UMAP representation of transcript levels for the indicated marker genes for (**C**) endothelial cells, (**D**) EMPs, (**E**) haematopoietic progenitors, and (**F**) erythroid cells. The scale bar represents log-normalised transcript levels.

Next, we integrated E-MTAB-11763 with E-MTAB-6967 to increase the number of cells available for downstream analysis in the haemato-vascular clusters to identify yolk sac haemogenic endothelium. As cells derived from the yolk sac and embryo proper had not been separately sequenced to generate E-MTAB-6967, we used a validated, reference-based annotation method [25] to harmonise cell type annotations and distinguish cells from these sources before integrating the two datasets (Figure 3A). Specifically, this method uses gene expression information to assign the most likely cluster from a reference dataset to a query dataset, which in our case involved applying our revised annotation for E8.5 data in E-MTAB-11763 to the E8.5 data in E-MTAB-6967. This approach increased the overall number of haemato-vascular cells from 8453 to 12,351 for further analysis (Figure 3B). We also surveyed the expression of key known marker genes of the cell populations of interest to confirm the appropriate annotation of the integrated dataset (Figure 3C–F).

3.2. Identifying Yolk Sac Haemogenic ECs via Their Transcriptomic Signature

The haemogenic endothelium is a rare and transient population and, thus, difficult to study [37,38]. To identify haemogenic ECs within the yolk sac endothelial cluster, we subset EMPs and ECs from both the yolk sac and the embryo proper and re-clustered them to generate a new UMAP including only these cells, which was annotated according to our refined nomenclature. Using this approach, yolk sac ECs clustered in an intermediate position between embryo-derived ECs and EMPs and also split into two sub-clusters, one positioned closer to EMPs and the other closer to endocardial ECs (Figure 4A). The analysis of known marker genes showed that both sub-clusters expressed markers of yolk sac endothelium at similar levels (*Lyve1* and *Stab2*), whereas only the EMP-proximal sub-cluster co-expressed haematopoietic progenitor genes (*Runx1*, *Myb*, and *Spi1*) (Figure 4B). Together, these findings indicate that a subset of yolk sac ECs have a dual endothelial and haematopoietic cell identity, consistent with a presumed identity of haemogenic ECs that give rise to EMPs.

3.3. Pseudotime Analysis Identifies Transcriptomic Changes Accompanying EHT

Having identified a cell cluster with haemogenic endothelial identity, we next used our refined annotation of the yolk sac populations to study signalling pathways and markers defining the transition from haemogenic ECs into EMPs and BPs. When analysing samples that contain cells along a continuous differentiation process, single-cell transcriptomic data can be used to arrange cells along a pseudotime trajectory [39]. In essence, pseudotime analysis uses gene expression patterns to reorder cells and arrange them based on their presumed progressive gene expression differences, thus reconstructing trajectories along which cells may be differentiating. Thus, we used pseudotime analysis of yolk sac cell populations to study the transition of ECs into haematopoietic populations. In agreement with prior knowledge of EHT, pseudotime analysis of our integrated E8.5 dataset suggested a continuum of cell differentiation from endothelial to haemogenic endothelium and then to haematopoietic cells (Figure 5A) and also highlighted progressive erythroid maturation (Figure 5B). A refined pseudotime analysis after exclusion of erythroid cells as the predominant cell type corroborated the expected progressive transition of yolk sac ECs to haemogenic ECs, EMPs, BP1, and BP2 (Figure 5C).

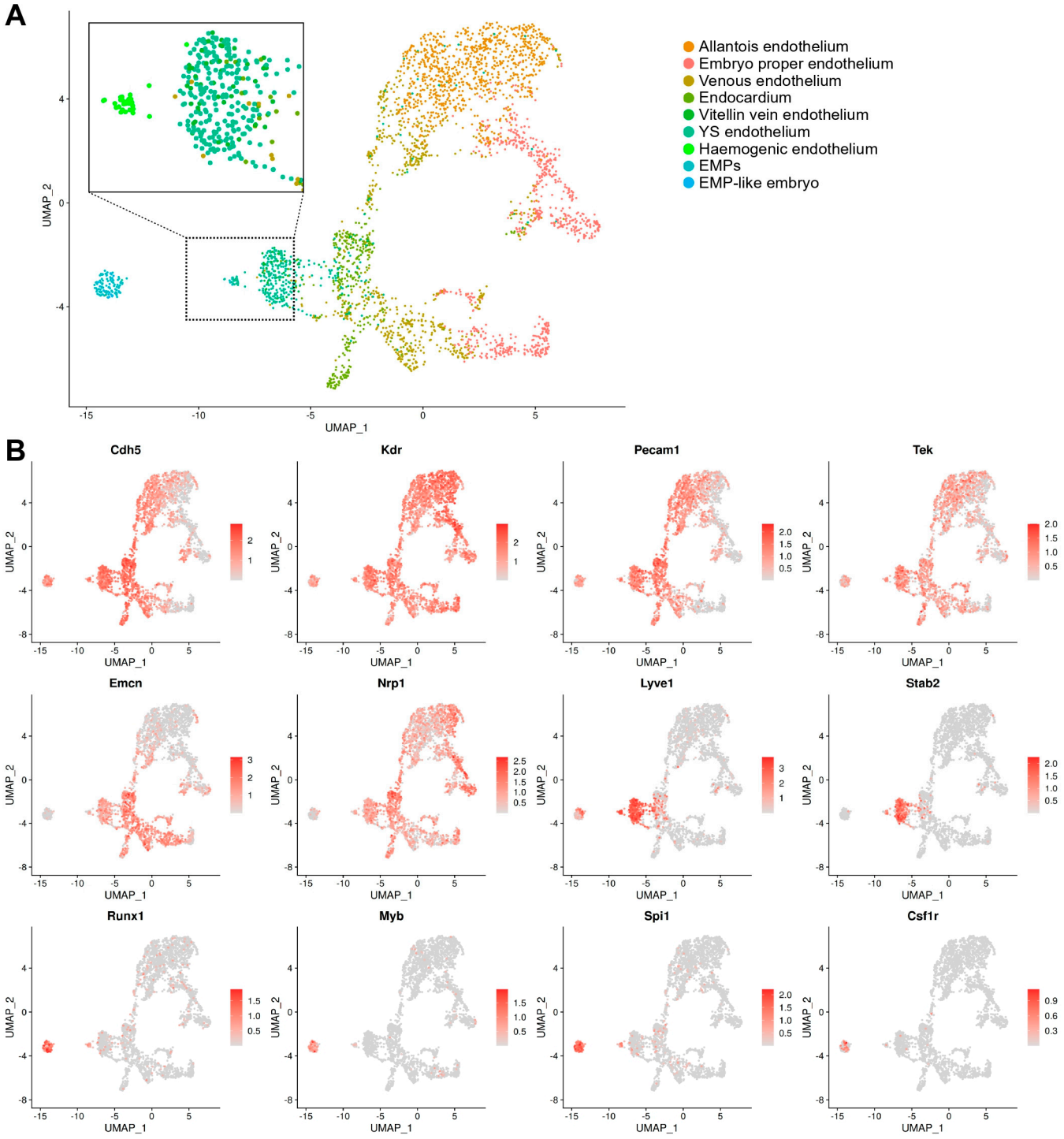

Figure 4. Endothelial cell and EMP sub-clustering identifies haemogenic endothelium. (**A**) UMAP obtained after subsetting and re-clustering all cells annotated as endothelial cells and EMPs after integration of E8.5 data in E-MTAB-11763 and E-MTAB-6967. The dotted box indicates an area that is zoomed on the cells previously annotated as yolk sac endothelial cells, vitellin vein endothelial cells, and EMPs; note the formation of a separate cluster positioned between EMPs and the main yolk sac endothelial cluster, consistent with a haemogenic endothelial identity. (**B**) UMAP representation of key endothelial and haematopoietic markers corroborates the identification of the haemogenic endothelial cluster. The scale bars represent log-normalised transcript levels. YS: yolk sac; EMPs: erythro-myeloid progenitors.

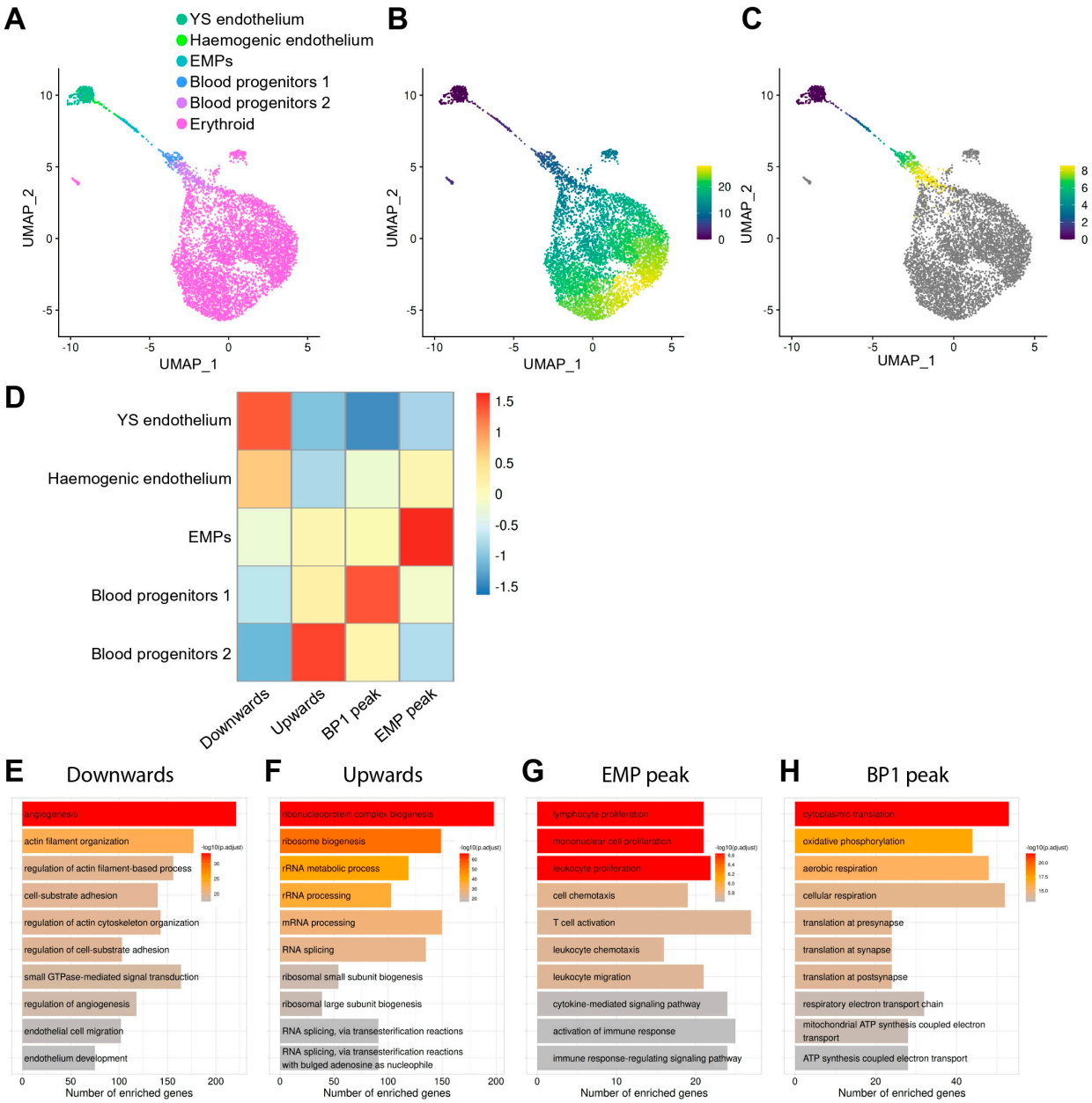

Figure 5. Pseudotime analysis identifies co-regulated genes and enriched GO pathways during EHT. (**A**) UMAP obtained after subsetting and re-clustering yolk sac haemato-vascular cells after integration of E8.5 data in E-MTAB-11763 and E-MTAB-6967 and showing our refined cluster annotation. (**B**,**C**) Pseudotime analysis highlights erythroid generation and progressive maturation (**B**) and, after excluding the erythroid cluster (**C**), the progressive differentiation from yolk sac endothelial cells to haemogenic endothelial cells and then EMPs, followed by blood progenitors 1 and 2. The scale bars represent pseudotime. (**D**) Genes that changed as a function of pseudotime were identified and grouped according to their expression patterns. The heatmap shows four groups of co-regulated genes during differentiation from yolk sac endothelium to blood progenitors 2. (**E**–**H**) Gene ontology analysis for each group of co-regulated genes. YS: yolk sac; EMP: erythro-myeloid progenitor; BP1: blood progenitors 1.

Next, we took advantage of a method that analyses genes that change as a function of pseudotime [40] to identify genes that showed an upward or downward trend during EHT (Figure 5D, Table S1). We found that 2924 genes were progressively downregulated, whereas 1776 genes were progressively upregulated, during the predicted transition from endothelial to haematopoietic cells. We also found that 231 genes were upregulated

during the predicted transition from ECs to EMPs but downregulated during subsequent differentiation towards BP1 and then BP2 (peak transcript levels in EMPs). Moreover, 848 genes were progressively upregulated from ECs to BP1 but downregulated in BP2 (peak transcript levels in BP1) (Figure 5D).

To identify potential biological processes underpinning EHT, we used gene ontology (GO) analysis on these four groups of co-regulated genes (Figure 5E–H, Table S2). The GO analysis of genes with a downward expression trend during the predicted progression from endothelial to haematopoietic cells revealed enrichment in biological processes related to angiogenesis, cytoskeleton re-organisation, cell adhesion, endothelial cell migration, and endothelial development (Figure 5E). Genes with an upward expression trend instead were involved in mRNA processing, splicing, and ribonucleoprotein biogenesis (Figure 5F). Genes that peaked in EMPs showed enrichment in terms involved in leukocyte migration, myeloid proliferation, and immune response (Figure 5G), in agreement with EMPs being responsible for the production of foetal blood and immune cells. Finally, genes that peaked in BP1 are involved in oxidative phosphorylation, cellular respiration, and ATP synthesis (Figure 5H), raising the possibility that these cells have increased metabolism.

To identify genes belonging to known signalling pathways amongst each one of the four groups of co-regulated genes, we performed pathway analysis using the WikiPathways resource [41] (Table S3). Genes that were downregulated when ECs were predicted to transition to haematopoietic cells belonged to the cholesterol biosynthesis, IL3, IL17A, PI3K/AKT/mTOR, and EFGR1 signalling pathways. Genes that were upregulated during this transition are involved in RNA processing and cell cycle activation. Genes peaking in BP1 are involved in the regulation of cell metabolism, whereas genes peaking in EMPs belonged to the TYROBP and IL5 signalling pathways (Table S3). Notably, by comparing EMPs to other yolk sac clusters, we identified multiple genes within the TYROBP signalling pathway that, in addition to peaking in EMPs, were significantly enriched in EMPs compared to the other cells in the haemato-vascular clusters (Figure S2).

Overall, this analysis provides insights into molecular changes predicted to accompany EHT and haematopoietic differentiation in the yolk sac and identifies candidate signalling pathways that may be studied further to understand the molecular control of these complex cellular differentiation pathways.

3.4. Differential Expression Analysis Identifies EMP and Haemogenic Endothelium Markers

To identify markers for haemogenic ECs and EMPs, we used our integrated E8.5 mouse dataset to perform differential expression (DE) analysis of endothelial and haematopoietic cell populations in both the yolk sac and embryo. First, we subset the clusters for both cell populations and then performed DE analyses by comparing clusters in different combinations to identify the top differentially regulated genes. To identify genes that may encode markers useful for cell identification via immunostaining or flow cytometric cell sorting, we filtered DE genes for those that encoded transmembrane proteins (Table S4).

By comparing EMPs to haematopoietic and endothelial cells, we identified *Csf1r* and *Alox5ap* as enriched in EMPs (Figure 6A), agreeing with previous studies that identified them as EMP markers [7,40]. In addition, we identified *Fcer1g*, *Tyrobp,* and *Mctp1* as potential new markers for EMPs (Figure 6A,B), whereas *Fxyd5* and *Scarf1* were identified as markers of yolk sac ECs and EMPs, and to a lesser extent of BP1 (Figure 6B). None of these seven genes was expressed in more differentiated BP2 and erythroid cells. A comparison of genes expressed in haemogenic ECs versus EMPs showed that acquisition of an EMP identity was associated with a loss of *Stab2* (Figure 6C), as previously described [35]. Furthermore, we identified *Icam2*, *Cldn5,* and *Gpr182* as additional genes that were expressed in yolk sac ECs and haemogenic ECs but downregulated in EMPs (Figure 6C).

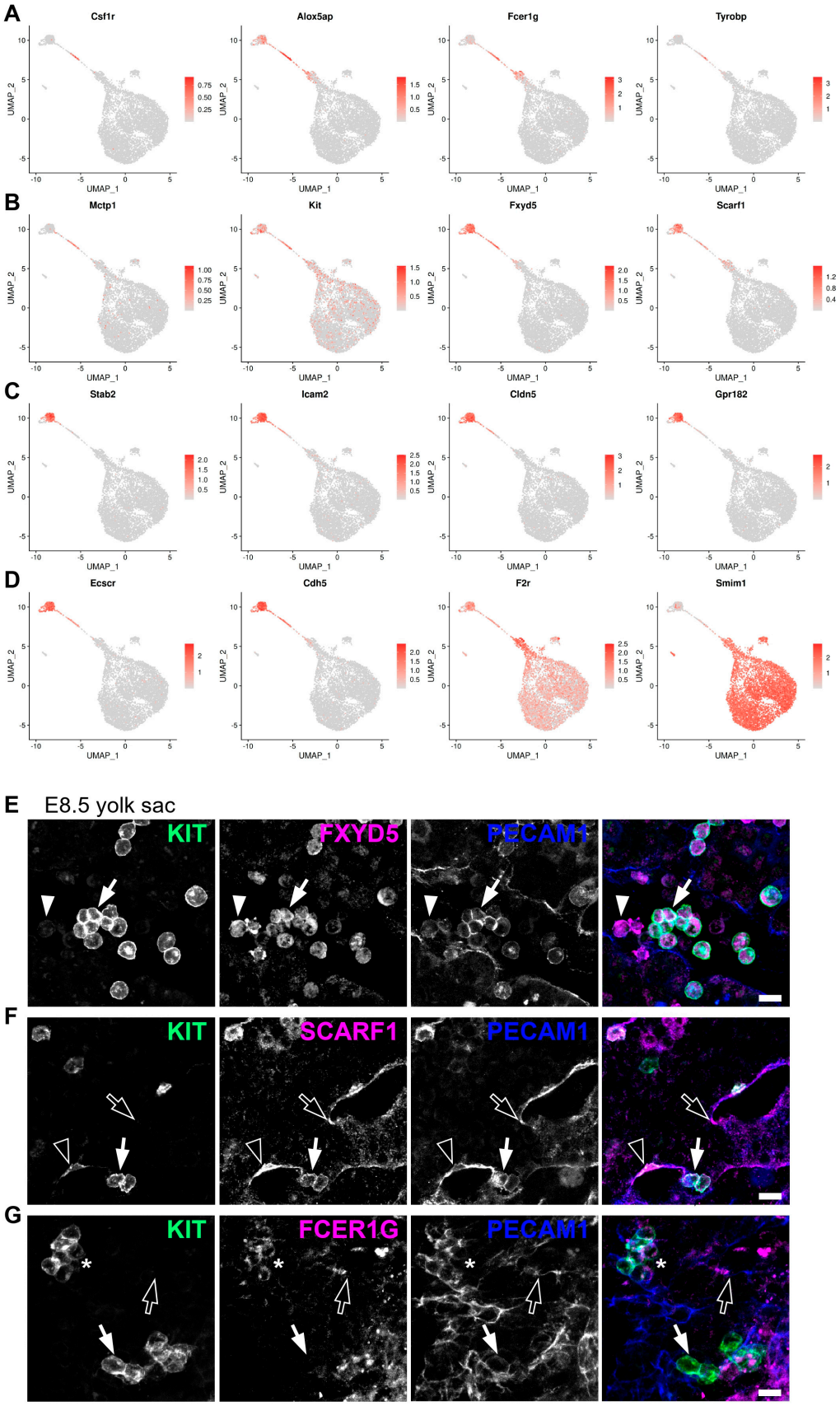

Figure 6. Differential gene (DE) expression analysis and immunostaining validation identify new markers for haemogenic endothelial cells and EMPs. (**A**–**D**) UMAP representation of transcript levels for the indicated marker genes identified by DE analysis between the different yolk sac haemato-vascular clusters. The scale bars represent log-normalised transcript levels. (**E**–**G**) Immunofluorescence staining

of E8.5 yolk sac for the EMP marker KIT together with PECAM1 and FXYD5, SCARF1, or FCER1G. Emerging EMPs are indicated with arrows (round KIT$^+$ PECAM1$^+$ cells), presumed blood (myeloid) progenitors with arrowheads (round KIT$^-$ PECAM1^{low} cells), endothelial cells with empty arrows (flat KIT$^-$ PECAM1$^+$ cells), haemogenic endothelial cells with empty arrowheads (flat KIT$^+$ PECAM1$^+$ cells), and mature EMPs with an asterisk (round KIT$^+$ PECAM1$^+$ FCER1G$^+$ cells). Scale bars: 50 µm; n = 3 embryos.

By comparing EMPs to BP1 and BP1 to BP2, we identified transcriptional changes associated with the EMP transition to more committed progenitor states. This transition was associated with the downregulation of the endothelial genes *Ecscr* and *Cdh5*, the EMP marker *Alox5ap*, as well as the downregulation of our predicted novel EMP marker *Fcer1g* and yolk sac EC and EMP markers *Fxyd5* and *Scarf1* (Figure 6A–D). By contrast, the EMP transition to more committed progenitor states was associated with the upregulation of the megakaryocytic gene *F2r* and the erythroid gene *Smim1* (Figure 6D).

To confirm that *Fxyd5*, *Scarf1,* and *Fcer1g* encode EMP and haemogenic endothelial markers, we performed immunofluorescence staining of the E8.5 yolk sac. Although we had found *Fxyd5* transcripts in yolk sac ECs and EMPs, FXYD5 staining was restricted to round KIT$^+$ PECAM1$^+$ cells consistent with newly emerging EMPs, and there was no obvious staining of ECs (Figures 6E and S3A). Additionally, FXYD5 immunostaining identified round KIT$^-$ PECAM1^{low} cells, agreeing with our transcriptomic analysis detecting BPs with no *Kit* transcripts and low levels of *Fxyd5* (Figure 6B). Consistent with the presence of *Scarf1* transcripts in both yolk sac ECs and EMPs, immunofluorescence staining identified SCARF1 protein in flat KIT$^-$ PECAM1$^+$ ECs and round KIT$^+$ PECAM1$^+$ emerging EMPs. Furthermore, SCARF1 immunostaining identified flat KIT$^+$ PECAM1$^+$ cells that may be haemogenic ECs (Figures 6F and S3B). Although *Fcer1g* transcripts were detected in both EMPs and BP1, immunofluorescence identified FCER1G protein within a subset of round KIT$^+$ cells. Additionally, FCER1G immunostaining identified flat KIT$^-$ PECAM1$^+$ ECs, consistent with our transcriptomic analysis detecting low levels of *Fcer1g* transcripts in yolk sac ECs (Figures 6G and S3C).

A comparison with clusters from the embryo showed that the markers identified in our analysis as expressed in yolk sac ECs (*Fxyd5*, *Scarf1*, *Icam2*, *Cldn5*, and *Gpr182*) were also detected in the endocardium and in venous ECs (Figure 7A–C). In contrast, the EMP markers we identified (*Csf1r*, *Alox5ap*, *Fcer1g*, *Tyrobp*, and *Mctp1*) were not expressed in ECs from the embryo, confirming their specificity. Nevertheless, these markers were also expressed in EMP-like cells from the embryo, thus corroborating their appropriate annotation.

Taken together, these findings show that novel EMP markers can be identified by scRNAseq analysis and that they could be used to investigate both bona fide EMPs in the yolk sac as well as poorly characterised EMP-like cells found in the embryo.

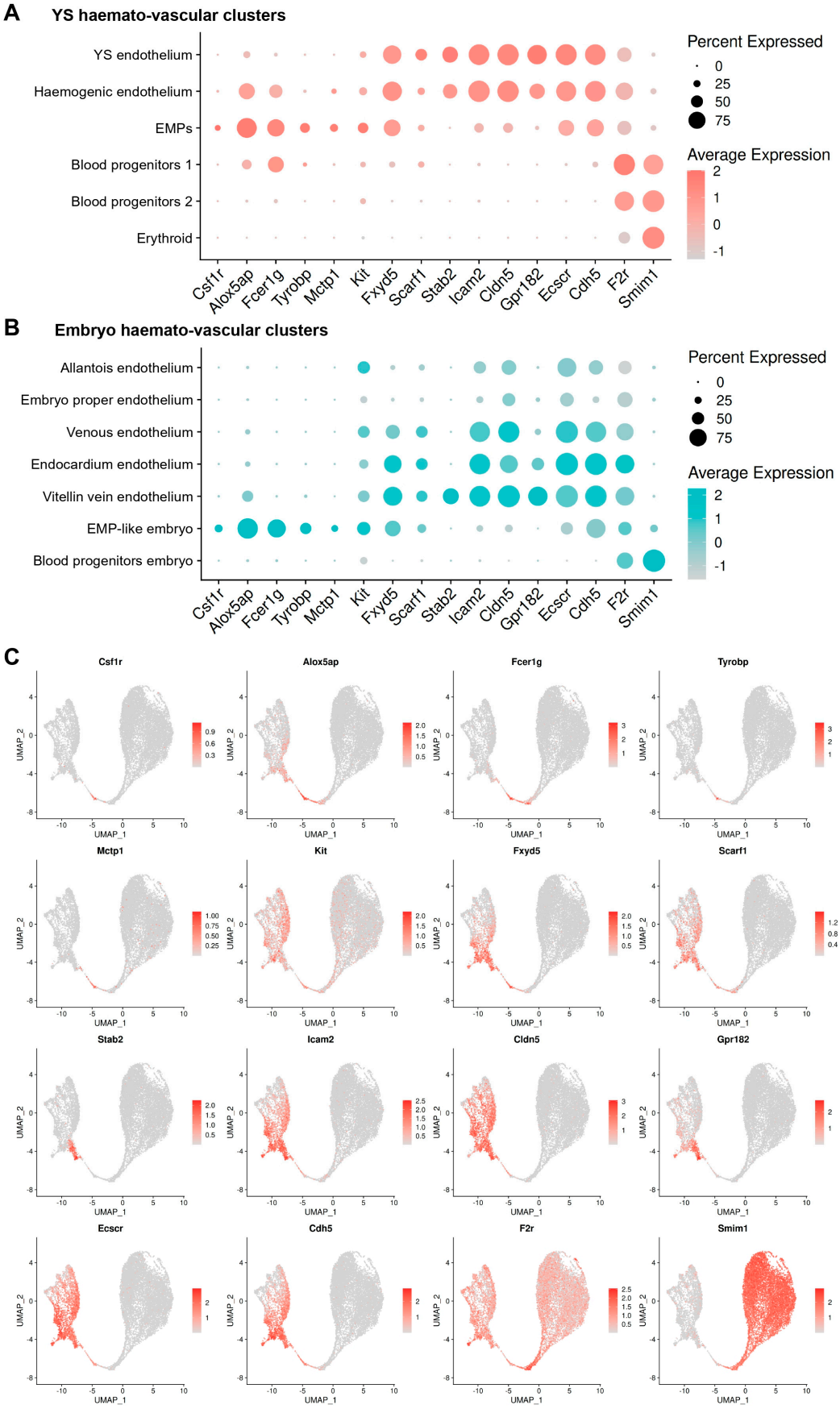

Figure 7. Expression analysis in haemato-vascular cells from both yolk sac and embryo shows the specificity of the new markers for haemogenic ECs and EMPs. (**A**,**B**) Dot plot representation of markers identified by DE analysis in (**A**) yolk sac and (**B**) embryo haemato-vascular clusters. The dot

size reflects the percentage of cells in each cluster expressing the gene. The scale bar indicates log-normalised gene expression. (**C**) UMAP of the E8.5 haemato-vascular clusters from both embryo and yolk sac showing transcript levels for the indicated markers identified by DE analysis. The scale bars represent log-normalised transcript levels.

4. Discussion

To capture the time when EMPs emerge from the yolk sac haemogenic endothelium and to define the transcriptome of the cell populations involved in EHT, we re-analysed transcriptomic data from the E8.5 mouse embryo (Figure 1). Our analysis provided a refined annotation of endothelial and haematopoietic populations in the mouse yolk sac (Figure 3A,B) and identified a subset of ECs co-expressing endothelial and haematopoietic markers, consistent with a haemogenic endothelial phenotype (Figure 4A,B). This refined annotation also defined E8.5 yolk sac EMPs and demonstrated co-expression of myeloid, erythroid, and progenitor markers in this cluster, consistent with the known dual erythro-myeloid differentiation potential of EMPs. Moreover, we identified EMP-like cells within the E8.5 embryo proper, which have not been highlighted in prior transcriptomic studies of early haematopoiesis (Figure 3B). Knowing that haematopoietic cells enter the embryo only from E9.5, when the heart begins to beat to initiate blood circulation [4,42], we considered two possibilities to explain the existence of EMP-like cells in the embryo. On the one hand, these cells may represent yolk sac-derived haematopoietic progenitors that had contaminated the embryonic samples during dissection. On the other hand, it is conceivable that these cells represent EMP-like cells originating in the embryo rather than in the yolk sac. The latter possibility is consistent with our recent discovery of a *Pax3* lineage-derived EMP-like progenitor in the mouse embryo [8]. However, further work is required to accurately describe these EMP-like cells.

Others have used scRNAseq to map potential differentiation trajectories for EMPs in the yolk sac [43]. Additionally, our analysis identified distinct BP1 and BP2 clusters as consecutive stages of EMP maturation (Figure 5A–C) and provided new insights into candidate signalling pathways controlling this transition (Figure 5D–H). As primitive erythrocytes are produced from E7.0 onwards [3,44], but EMPs only emerge from E8.5 onwards [5,7,18,20], the erythroid cluster in the E8.5 dataset is expected to contain mostly primitive erythrocytes that were produced prior to or alongside EMP emergence, with only a potential minor contribution from EMP-derived erythrocytes. No markers of fully differentiated macrophages or other myeloid cell types were observed, confirming previous studies showing that macrophages form in the yolk sac from E9.0 onwards [36]. We also did not detect a lymphoid cluster at E8.5, in agreement with prior reports of LMP presence in the yolk sac only from E9.5 onwards [6].

Previous studies established that EHT is associated with downregulation of endothelial genes and concomitant upregulation of haematopoietic genes [5,38,44–46]. Here, pseudotime reconstruction highlighted dynamic gene expression trends during EHT and haematopoietic maturation in the yolk sac (Figure 5A–D), whereby haemogenic ECs form a transcriptional continuum bridging the transition from endothelial to haematopoietic cell identities, thus implying a gradual and continuous process rather than a discrete lineage switch. Altogether, these findings align with established models of yolk sac haematopoiesis derived from genetic lineage tracing, flow cytometry experiments, and prior transcriptomic analysis [1,5,15,16,36].

The progressive downregulation of genes associated with angiogenesis, cytoskeletal organisation, and endothelial adhesion during the predicted EHT (Figure 5E) may indicate structural and functional changes necessary for cell detachment and transition to a haematopoietic phenotype. Conversely, the upregulation of genes associated with RNA

processing (Figure 5F) suggests that haematopoietic specification is coupled to enhanced transcriptional activity. Furthermore, upregulation of genes associated with cell cycle activation and transition from the G1 to S phase (Table S3) agrees with previous findings that EHT requires cell cycle progression and is controlled by the cell cycle regulators CDK4/6 and CDK1 [46,47].

DE analysis identified components of the TYROBP signalling pathway as significantly enriched in EMPs (Figure S2). In the adult, the activation of the TYROBP signalling pathway has been associated with the microglial response to stress [48,49]. However, to the best of our knowledge, this signalling pathway has not been previously associated with EMP emergence. Further investigation should determine whether this pathway may be functionally involved in the production of EMPs or other haematopoietic progenitors (e.g., HSCs from the dorsal aorta) and whether manipulating TYROBP in vitro during differentiation of induced pluripotent stem cells may allow to devise more efficient haematopoietic differentiation methods.

DE analysis also identified upregulation of genes associated with oxidative phosphorylation upon differentiation of EMPs to BP1 (Figure 5H). Previous studies of pluripotent stem cells and neuronal progenitors showed that their differentiation is associated with metabolic reprogramming, whereby differentiating progenitors switch from glycolysis to oxidative phosphorylation [50–52]. Our analysis raises the possibility that an analogous process may occur when haematopoietic progenitors in the yolk sac commit to differentiation.

Our DE analysis identified both known and previously undescribed candidate markers associated with the formation of haemogenic endothelium and EMPs (Figure 6A–D). Established EMP markers such as *Csf1r* and *Alox5ap* were previously described by others [7,40], thus validating the robustness of our transcriptomic analysis. In addition, we identified *Fcer1g*, *Tyrobp*, and *Mctp1* as potential novel EMP markers, and *Fxyd5* and *Scarf1* as shared markers between yolk sac endothelial and haematopoietic cells. The expression of *Fxyd5* and *Scarf1* in endothelial and EMP clusters, and to a lower extent in BP1, but not in more differentiated cells, suggests that these genes may serve as new markers for yolk sac ECs and emerging EMPs. Immunofluorescence staining of the E8.5 yolk sac corroborated the predictions of our DE analysis: FXYD5 was present on round KIT$^+$ PECAM1$^+$ cells consistent with emerging EMPs (Figures 6E and S3A); SCARF1 labelled flat KIT$^-$ PECAM1$^+$ ECs, flat KIT$^+$ PECAM1$^+$ cells consistent with haemogenic ECs and round KIT$^+$ PECAM1$^+$ cells consistent with emerging EMPs (Figures 6F and S3B); FCER1G marked flat KIT$^-$ PECAM1$^+$ ECs and a few round KIT$^+$ PECAM1$^+$ cells that may represent a subset of EMPs (Figures 6G and S3C). Nevertheless, these experiments also highlighted differences in RNA and protein expression. Thus, although *Fxyd5* RNA was detected in yolk sac ECs, haemogenic ECs, and EMPs, and at lower levels in BP1, the FXYD5 protein appeared to be prevalent in round KIT$^+$ PECAM1$^+$ cells consistent with EMPs and in round KIT$^-$ PECAM1^{low} cells presumed to be myeloid-committed BP1 (Figures 6E and S3A). While *Fcer1g* RNA clearly identified the EMP cluster, the FCER1G protein was detected in only a subset of round KIT$^+$ PECAM1$^+$ cells, possibly marking more mature EMPs (Figures 6G and S3C). This is reminiscent of observations for *Csf1r*, a gene expressed in EMPs at the RNA level, whereas CSF1R protein only becomes translated upon differentiation to myeloid cells [7]. These discrepancies between RNA and protein expression may be due to differences in expression dynamics and half-lives for mRNAs and proteins [53]. Overall, these immunostaining results validated our transcriptomic predictions and highlighted the utility of single-cell datasets in discovering functional cell surface markers. Previously used markers for haemogenic ECs include the surface markers CDH5, KIT, and CD41, and haematopoietic transcription factors such as RUNX1 [45,54,55], whereas previously used markers for EMPs include KIT, CD41, and CD16/32, as well as the gene

expression reporter *Csf1r*-eGFP [56–58]. The addition of the novel markers identified in our analysis will provide complementary tools to define haemogenic ECs and EMPs in the mouse yolk sac. Future studies should test these markers in flow cytometry panels, for example to validate their usefulness for isolating haemogenic endothelial cells and haematopoietic progenitors and to examine whether their use allows isolation of progenitor subpopulations with higher specificity compared to currently available strategies, for example when performing clonogenic assays. In summary, this study refines the cellular and molecular characterisation of yolk sac haematopoiesis, provides a detailed transcriptomic roadmap of EHT in the yolk sac, and identifies novel candidate markers for haemogenic endothelium and EMPs. The identification of FXYD5, SCARF1, and FCER1G as markers for EMPs and haemogenic ECs may offer valuable tools for future in vivo and in vitro studies. Finally, future studies may wish to determine whether the novel EMP markers are present also in foetal HSCs and whether they are conserved in human haemopoiesis. Defining the specificity of such novel markers may allow researchers to better define EMP identity and lineage potential as a prerequisite for deciphering the ontogeny of the immune system and, ultimately, to harness early haematopoietic pathways for regenerative medicine.

Supplementary Materials: The following supporting information can be downloaded at: https://www.mdpi.com/article/10.3390/jdb14010004/s1, Figure S1. Cluster annotation of E8.5 mouse scRNAseq data in E-MTAB-11763. UMAP of the E8.5 cells in E-MTAB-11763 dataset, labelled with the cluster annotations provided by the authors of the original publication [22]. Figure S2. The TYROBP signalling pathway is enriched in emerging EMPs. TYROBP pathway genes enriched in EMPs compared to haemato-vascular clusters from both yolk sac and embryo. The box colour indicates the average log2 fold change. A green border indicates significant enrichment in EMPs. Figure S3. Immunostaining validation of new markers for haemogenic endothelial cells and EMPs. (A–C) Immunofluorescence staining of E8.5 yolk sac for the EMP marker KIT together with PECAM1 and FXYD5, SCARF1 or FCER1G. Emerging EMPs are indicated with arrows (round KIT^+ $PECAM1^+$ cells), presumed blood (myeloid) progenitors with arrowheads (round KIT^- $PECAM1^{low}$ cells), endothelial cells with empty arrows (flat KIT^- $PECAM1^+$ cells), haemogenic endothelial cells with empty arrowheads (flat KIT^+ $PECAM1^+$ cells) and mature EMPs with asterisk (round KIT^+ $PECAM1^+$ $FCER1G^+$ cells). Scale bars: 50 μm; $n = 3$ embryos. Table S1. Genes that change as a function of pseudotime, showing an upward or downward trend during EHT, or peaking in either EMPs or BP1. Table S2. List of biological processes identified through gene ontology (GO) analysis on the four groups of genes that are co-regulated during EHT. Table S3. Signalling pathways identified though the WikiPathways resource to identify genes belonging to known signalling pathways amongst each one of the four groups of genes that are co-regulated during EHT. Table S4. List of genes that are differentially expressed between endothelial and haematopoietic cell populations in both the yolk sac and embryo, and filtered for genes encoding transmembrane proteins.

Author Contributions: G.C., G.D.-P. and C.R. conceived and designed the study. G.C. and C.R. co-wrote the manuscript. G.C. and A.M. performed immunostaining experiments. G.D.-P. performed bioinformatic analyses. G.C. and C.R. supervised the project. All authors have read and agreed to the published version of the manuscript.

Funding: This research was funded by a Wellcome grant [205099/Z/16/Z] and a British Heart Foundation grant [PG23/11301].

Data Availability Statement: The data presented in this study are available in ArrayExpress at https://www.ebi.ac.uk/biostudies/arrayexpress/, reference number E-MTAB-6967 and E-MTAB-11763. These data were derived from the following resources available in the public domain: https://www.ebi.ac.uk/biostudies/arrayexpress/studies/E-MTAB-6967 and https://www.ebi.ac.uk/biostudies/arrayexpress/studies/E-MTAB-11763 (last accessed on 25 August 2025).

Acknowledgments: We thank the staff of the Biological Resources, FACS, and Imaging Facilities at the UCL Institute of Ophthalmology for their technical support.

Conflicts of Interest: The authors declare no conflicts of interest.

References

1. Canu, G.; Ruhrberg, C. First blood: The endothelial origins of hematopoietic progenitors. *Angiogenesis* **2021**, *24*, 199–211. [CrossRef]
2. Ivanovs, A.; Rybtsov, S.; Ng, E.S.; Stanley, E.G.; Elefanty, A.G.; Medvinsky, A. Human haematopoietic stem cell development: From the embryo to the dish. *Development* **2017**, *144*, 2323–2337. [CrossRef]
3. Ferkowicz, M.J.; Yoder, M.C. Blood island formation: Longstanding observations and modern interpretations. *Exp. Hematol.* **2005**, *33*, 1041–1047. [CrossRef] [PubMed]
4. Frame, J.M.; Fegan, K.H.; Conway, S.J.; McGrath, K.E.; Palis, J. Definitive Hematopoiesis in the Yolk Sac Emerges from Wnt-Responsive Hemogenic Endothelium Independently of Circulation and Arterial Identity. *Stem Cells* **2016**, *34*, 431–444. [CrossRef] [PubMed]
5. Frame, J.M.; McGrath, K.E.; Palis, J. Erythro-myeloid progenitors: "definitive" hematopoiesis in the conceptus prior to the emergence of hematopoietic stem cells. *Blood Cells Mol. Dis.* **2013**, *51*, 220–225. [CrossRef] [PubMed]
6. Böiers, C.; Carrelha, J.; Lutteropp, M.; Luc, S.; Green, J.C.; Azzoni, E.; Woll, P.S.; Mead, A.J.; Hultquist, A.; Swiers, G.; et al. Lymphomyeloid Contribution of an Immune-Restricted Progenitor Emerging Prior to Definitive Hematopoietic Stem Cells. *Cell Stem Cell* **2013**, *13*, 535–548. [CrossRef] [PubMed]
7. Hoeffel, G.; Chen, J.; Lavin, Y.; Low, D.; Almeida, F.F.; See, P.; Beaudin, A.E.; Lum, J.; Low, I.; Forsberg, E.C.; et al. C-Myb+ Erythro-Myeloid Progenitor-Derived Fetal Monocytes Give Rise to Adult Tissue-Resident Macrophages. *Immunity* **2015**, *42*, 665–678. [CrossRef]
8. Canu, G.; Correra, R.; Diez-Pinel, G.; Castellan, R.F.P.; Denti, L.; Fantin, A.; Ruhrberg, C. A Pax3 lineage gives rise to transient haematopoietic progenitors. *Development* **2024**, *151*, dev202924. [CrossRef]
9. Liu, X.; Ren, Z.; Tan, C.; Núñez-Santana, F.L.; Kelly, M.E.; Yan, Y.; Sun, H.; Abdala-Valencia, H.; Yang, W.; Wu, Q.; et al. Inducible CCR2+ nonclassical monocytes mediate the regression of cancer metastasis. *J. Clin. Investig.* **2024**, *134*, e179527. [CrossRef]
10. Jiang, Y.; Cai, R.; Huang, Y.; Zhu, L.; Xiao, L.; Wang, C.; Wang, L. Macrophages in organ fibrosis: From pathogenesis to therapeutic targets. *Cell Death Discov.* **2024**, *10*, 487. [CrossRef]
11. Moskalik, A.; Niderla-Bielińska, J.; Ratajska, A. Multiple roles of cardiac macrophages in heart homeostasis and failure. *Heart Fail. Rev.* **2021**, *27*, 1413. [CrossRef]
12. Tavian, M.; Tavian, M.; Coulombel, L.; Luton, D.; Clemente, H.S.; Dieterlen-Lièvre, F.; Peault, B. Aorta-Associated CD34+ Hematopoietic Cells in the Early Human Embryo. *Blood* **1996**, *87*, 67–72. [CrossRef]
13. Oberlin, E.; El Hafny, B.; Petit-Cocault, L.; Souyri, M. Definitive human and mouse hematopoiesis originates from the embryonic endothelium: A new class of HSCs based on VE-cadherin expression. *Int. J. Dev. Biol.* **2010**, *54*, 1165–1173. [CrossRef]
14. Ivanovs, A.; Rybtsov, S.; Welch, L.; Anderson, R.A.; Turner, M.L.; Medvinsky, A. Highly potent human hematopoietic stem cells first emerge in the intraembryonic aorta-gonad-mesonephros region. *J. Exp. Med.* **2011**, *208*, 2417–2427. [CrossRef] [PubMed]
15. Sánchez-Lanzas, R.; Jiménez-Pompa, A.; Ganuza, M. The evolving hematopoietic niche during development. *Front. Mol. Biosci.* **2024**, *11*, 1488199. [CrossRef] [PubMed]
16. Sugimura, R.; Fidanza, A.; Azzoni, E.; Canu, G. Editorial: Plasticity of the haematopoietic niche: From embryonic development to aging and disease. *Front. Mol. Biosci.* **2025**, *12*, 1683902. [CrossRef] [PubMed]
17. Van Deren, D.A.; De, S.; Xu, B.; Eschenbacher, K.M.; Zhang, S.; Capecchi, M.R. Defining the Hoxb8 cell lineage during murine definitive hematopoiesis. *Development* **2022**, *149*, dev200200. [CrossRef]
18. McGrath, K.E.; Frame, J.M.; Fegan, K.H.; Bowen, J.R.; Conway, S.J.; Catherman, S.C.; Kingsley, P.D.; Koniski, A.D.; Palis, J. Distinct sources of hematopoietic progenitors emerge before HSCs and provide functional blood cells in the mammalian embryo. *Cell Rep.* **2015**, *11*, 1892. [CrossRef]
19. McGrath, K.E.; Frame, J.M.; Palis, J. Early hematopoiesis and macrophage development. *Semin. Immunol.* **2016**, *27*, 379. [CrossRef]
20. Gomez Perdiguero, E.; Klapproth, K.; Schulz, C.; Busch, K.; Azzoni, E.; Crozet, L.; Garner, H.; Trouillet, C.; de Bruijn, M.F.; Geissmann, F.; et al. Tissue-resident macrophages originate from yolk-sac-derived erythro-myeloid progenitors. *Nature* **2014**, *518*, 547–551. [CrossRef]
21. Pijuan-Sala, B.; Griffiths, J.A.; Guibentif, C.; Hiscock, T.W.; Jawaid, W.; Calero-Nieto, F.J.; Mulas, C.; Ibarra-Soria, X.; Tyser, R.C.; Ho, D.L.L.; et al. A single-cell molecular map of mouse gastrulation and early organogenesis. *Nature* **2019**, *566*, 490–495. [CrossRef] [PubMed]

22. Goh, I.; Botting, R.A.; Rose, A.; Webb, S.; Engelbert, J.; Gitton, Y.; Stephenson, E.; Londoño, M.Q.; Mather, M.; Mende, N.; et al. Yolk sac cell atlas reveals multiorgan functions during human early development. *Science* **2023**, *381*, eadd7564. [CrossRef] [PubMed]
23. Satija, R.; Farrell, J.A.; Gennert, D.; Schier, A.F.; Regev, A. Spatial reconstruction of single-cell gene expression data. *Nat. Biotechnol.* **2015**, *33*, 495–502. [CrossRef]
24. Korsunsky, I.; Millard, N.; Fan, J.; Slowikowski, K.; Zhang, F.; Wei, K.; Baglaenko, Y.; Brenner, M.; Loh, P.-R.; Raychaudhuri, S. Fast, sensitive and accurate integration of single-cell data with Harmony. *Nat. Methods* **2019**, *16*, 1289–1296. [CrossRef]
25. Aran, D.; Looney, A.P.; Liu, L.; Wu, E.; Fong, V.; Hsu, A.; Chak, S.; Naikawadi, R.P.; Wolters, P.J.; Abate, A.R.; et al. Reference-based analysis of lung single-cell sequencing reveals a transitional profibrotic macrophage. *Nat. Immunol.* **2019**, *20*, 163–172. [CrossRef]
26. Cao, J.; Spielmann, M.; Qiu, X.; Huang, X.; Ibrahim, D.M.; Hill, A.J.; Zhang, F.; Mundlos, S.; Christiansen, L.; Steemers, F.J.; et al. The single-cell transcriptional landscape of mammalian organogenesis. *Nature* **2019**, *566*, 496–502. [CrossRef]
27. Wu, T.; Hu, E.; Xu, S.; Chen, M.; Guo, P.; Dai, Z.; Feng, T.; Zhou, L.; Tang, W.; Zhan, L.; et al. clusterProfiler 4.0: A universal enrichment tool for interpreting omics data. *Innovation* **2021**, *2*, 100141. [CrossRef]
28. Shannon, P.; Markiel, A.; Ozier, O.; Baliga, N.S.; Wang, J.T.; Ramage, D.; Amin, N.; Schwikowski, B.; Ideker, T. Cytoscape: A Software Environment for Integrated Models of Biomolecular Interaction Networks. *Genome Res.* **2003**, *13*, 2498. [CrossRef]
29. Gustavsen, J.A.; Pai, S.; Isserlin, R.; Demchak, B.; Pico, A.R. RCy3: Network biology using Cytoscape from within R. *F1000Research* **2019**, *8*, 1774. [CrossRef]
30. Carlson, M. org.Mm.eg.db—Genome wide annotation for Mouse, Bioconductor. 2025. Available online: https://bioconductor.org/packages/release/data/annotation/manuals/org.Mm.eg.db/man/org.Mm.eg.db.pdf (accessed on 30 July 2025).
31. Pagès, H.; Carlson, M.; Falcon, S.; Li, N. AnnotationDbi—Manipulation of SQLite-Based annotations in Bioconductor, Bioconductor. 2025. Available online: https://bioconductor.org/packages/devel/bioc/manuals/AnnotationDbi/man/AnnotationDbi.pdf (accessed on 30 July 2025).
32. Marsh, S.; Tang, M.; Kozareva, V.; Graybuck, L.; Clarke, Z. scCustomize: Custom Visualizations & Functions for Streamlined Analyses of Single Cell Sequencing, CRAN: Contributed Packages. 2025. Available online: https://rdrr.io/cran/scCustomize/ (accessed on 30 July 2025).
33. Wickham, H.; Chang, W.; Henry, L.; Takahashi, K.; Wilke, C.; Woo, K.; Yutani, H.; Dunnington, D.; van den Brand, T. ggplot2: Create Elegant Data Visualisations Using the Grammar of Graphics. CRAN: Contributed Packages [Preprint]. 2025. Available online: https://search.r-project.org/CRAN/refmans/ggplot2/html/ggplot2-package.html (accessed on 30 July 2025).
34. Gordon, E.J.; Gale, N.W.; Harvey, N.L. Expression of the hyaluronan receptor LYVE-1 is not restricted to the lymphatic vasculature; LYVE-1 is also expressed on embryonic blood vessels. *Dev. Dyn.* **2008**, *237*, 1901–1909. [CrossRef]
35. Shvartsman, M.; Pavlovich, P.V.; Oatley, M.; Ganter, K.; McKernan, R.; Prialgauskaite, R.; Adamov, A.; Chukreev, K.; Descostes, N.; Buness, A.; et al. Single-cell atlas of major haematopoietic tissues sheds light on blood cell formation from embryonic endothelium. *bioRxiv* **2019**, 774547. [CrossRef]
36. Hoeffel, G.; Ginhoux, F. Fetal monocytes and the origins of tissue-resident macrophages. *Cell. Immunol.* **2018**, *330*, 5–15. [CrossRef] [PubMed]
37. Scarfò, R.; Randolph, L.N.; Alezz, M.A.; El Khoury, M.; Gersch, A.; Li, Z.-Y.; Luff, S.A.; Tavosanis, A.; Ramondo, G.F.; Valsoni, S.; et al. CD32 captures committed haemogenic endothelial cells during human embryonic development. *Nat. Cell Biol.* **2024**, *26*, 719–730. [CrossRef] [PubMed]
38. Gritz, E.; Hirschi, K.K. Specification and function of hemogenic endothelium during embryogenesis. *Cell. Mol. Life Sci. CMLS* **2016**, *73*, 1547–1567. [CrossRef]
39. Cannoodt, R.; Saelens, W.; Saeys, Y. Computational methods for trajectory inference from single-cell transcriptomics. *Eur. J. Immunol.* **2016**, *46*, 2496–2506. [CrossRef]
40. Sharon, N.; Chawla, R.; Mueller, J.; Vanderhooft, J.; Whitehorn, L.J.; Rosenthal, B.; Gürtler, M.; Estanboulieh, R.R.; Shvartsman, D.; Gifford, D.K.; et al. A Peninsular Structure Coordinates Asynchronous Differentiation with Morphogenesis to Generate Pancreatic Islets. *Cell* **2019**, *176*, 790–804.e13. [CrossRef]
41. Agrawal, A.; Balcı, H.; Hanspers, K.; Coort, S.L.; Martens, M.; Slenter, D.N.; Ehrhart, F.; Digles, D.; Waagmeester, A.; Wassink, I.; et al. WikiPathways 2024: Next generation pathway database. *Nucleic Acids Res.* **2024**, *52*, D679–D689. [CrossRef]
42. Kasaai, B.; Caolo, V.; Peacock, H.M.; Lehoux, S.; Gomez-Perdiguero, E.; Luttun, A.; Jones, E.A.V. Erythro-myeloid progenitors can differentiate from endothelial cells and modulate embryonic vascular remodeling. *Sci. Rep.* **2017**, *7*, srep43817. [CrossRef]
43. Zhao, Y.X.; Song, J.; Bao, X.; Zhang, J.; Wu, J.; Wang, L.; He, C.; Shao, W.; Bai, X.; Liang, T.; et al. Single-cell RNA sequencing-guided fate-mapping toolkit delineates the contribution of yolk sac erythro-myeloid progenitors. *Cell Rep.* **2023**, *42*, 113364. [CrossRef]
44. Palis, J.; Robertson, S.; Kennedy, M.; Wall, C.; Keller, G. Development of erythroid and myeloid progenitors in the yolk sac and embryo proper of the mouse. *Development* **1999**, *126*, 5073–5084. [CrossRef]

45. Lilly, A.J.; Costa, G.; Largeot, A.; Fadlullah, M.Z.H.; Lie-A-Ling, M.; Lacaud, G.; Kouskoff, V. Interplay between SOX7 and RUNX1 regulates hemogenic endothelial fate in the yolk sac. *Development* **2016**, *143*, 4341–4351. [CrossRef] [PubMed]
46. Canu, G.; Athanasiadis, E.; Grandy, R.A.; Garcia-Bernardo, J.; Strzelecka, P.M.; Vallier, L.; Ortmann, D.; Cvejic, A. Analysis of endothelial-to-haematopoietic transition at the single cell level identifies cell cycle regulation as a driver of differentiation. *Genome Biol.* **2020**, *21*, 157. [CrossRef] [PubMed]
47. Marcelo, K.L.; Sills, T.M.; Coskun, S.; Vasavada, H.; Sanglikar, S.; Goldie, L.C.; Hirschi, K.K. Hemogenic endothelial cell specification requires c-Kit, notch signaling, and p27-mediated cell-cycle control. *Dev. Cell* **2013**, *27*, 504–515. [CrossRef]
48. Zhang, M.; Duan, Y.; Gan, H.; Jiang, N.; Qin, L.; Luo, Y.; Palahati, A.; He, Y.; Li, C.; Zhai, X. TYROBP serve as potential immune-related signature genes in the acute phase of intracerebral hemorrhage. *Sci. Rep.* **2024**, *14*, 20158. [CrossRef] [PubMed]
49. Haure-Mirande, J.V.; Audrain, M.; Ehrlich, M.E.; Gandy, S. Microglial TYROBP/DAP12 in Alzheimer's disease: Transduction of physiological and pathological signals across TREM2. *Mol. Neurodegener.* **2022**, *17*, 55. [CrossRef]
50. Mahmoud, A.I. Metabolic switches during development and regeneration. *Development* **2023**, *150*, dev202008. [CrossRef]
51. Dahan, P.; Lu, V.; Nguyen, R.M.T.; Kennedy, S.A.L.; Teitell, M.A. Metabolism in pluripotency: Both driver and passenger? *J. Biol. Chem.* **2019**, *294*, 5420–5429. [CrossRef]
52. Zheng, X.; Boyer, L.; Jin, M.; Mertens, J.; Kim, Y.; Ma, L.; Hamm, M.; Gage, F.H.; Hunter, T. Metabolic reprogramming during neuronal differentiation from aerobic glycolysis to neuronal oxidative phosphorylation. *eLife* **2016**, *5*, e13374. [CrossRef]
53. Vogel, C.; Marcotte, E.M. Insights into the regulation of protein abundance from proteomic and transcriptomic analyses. *Nat. Rev. Genet.* **2012**, *13*, 227–232. [CrossRef]
54. Mikkola, H.K.A.; Fujiwara, Y.; Schlaeger, T.M.; Traver, D.; Orkin, S.H. Expression of CD41 marks the initiation of definitive hematopoiesis in the mouse embryo. *Blood* **2003**, *101*, 508–516. [CrossRef]
55. Nadin, B.M.; Goodell, M.A.; Hirschi, K.K. Phenotype and hematopoietic potential of side population cells throughout embryonic development. *Blood* **2003**, *102*, 2436–2443. [CrossRef]
56. McGrath, K.E.; Fegan, K.H.; Frame, J.M.; Kingsley, P.D.; Palis, J. Definitive Erythro-Myeloid Progenitors (EMP) Emerge in the Yolk Sac From Hemogenic Endothelium and Share Transcriptional Regulators with Adult Hematopoiesis. *Blood* **2011**, *118*, 910. [CrossRef]
57. Azzoni, E.; Frontera, V.; McGrath, K.E.; Harman, J.; Carrelha, J.; Nerlov, C.; Palis, J.; Jacobsen, S.E.W.; de Bruijn, M.F. Kit ligand has a critical role in mouse yolk sac and aorta–gonad–mesonephros hematopoiesis. *EMBO Rep.* **2018**, *19*, e45477. [CrossRef]
58. Plein, A.; Fantin, A.; Denti, L.; Pollard, J.W.; Ruhrberg, C. Erythro-myeloid progenitors contribute endothelial cells to blood vessels. *Nature* **2018**, *562*, 223–228. [CrossRef]